Supporting Information

Inorganic $CuFeO_2$ Delafossite Nanoparticles as Effective Hole Transport Material for Highly Efficient and Long-Term Stable Perovskite Solar Cells

Seckin Akin[a,b,c], Faranak Sadegh[d], Servet Turan[c], Savas Sonmezoglu[a,b,*]

[a]Nanotechnology R&D Laboratory, Karamanoglu Mehmetbey University, Karaman, Turkey

[b]Department of Metallurgical and Materials Engineering, Karamanoglu Mehmetbey University, Karaman, Turkey

[c]Department of Materials Science and Engineering, Eskisehir Technical University, Eskisehir, Turkey

[d]Department of Chemistry, Catalysis Division, University of Isfahan, Isfahan 81746-73441, Iran

[*]E-mail address of corresponding author: svssonmezoglu@gmail.com

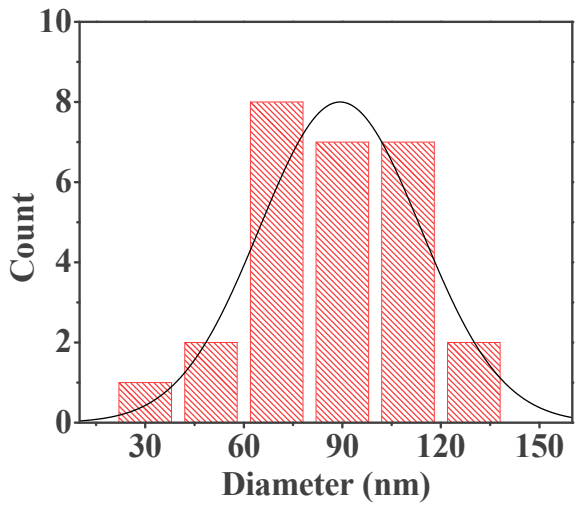

Fig. S1. Diameter distribution of CFO nanoparticles obtained from TEM image.

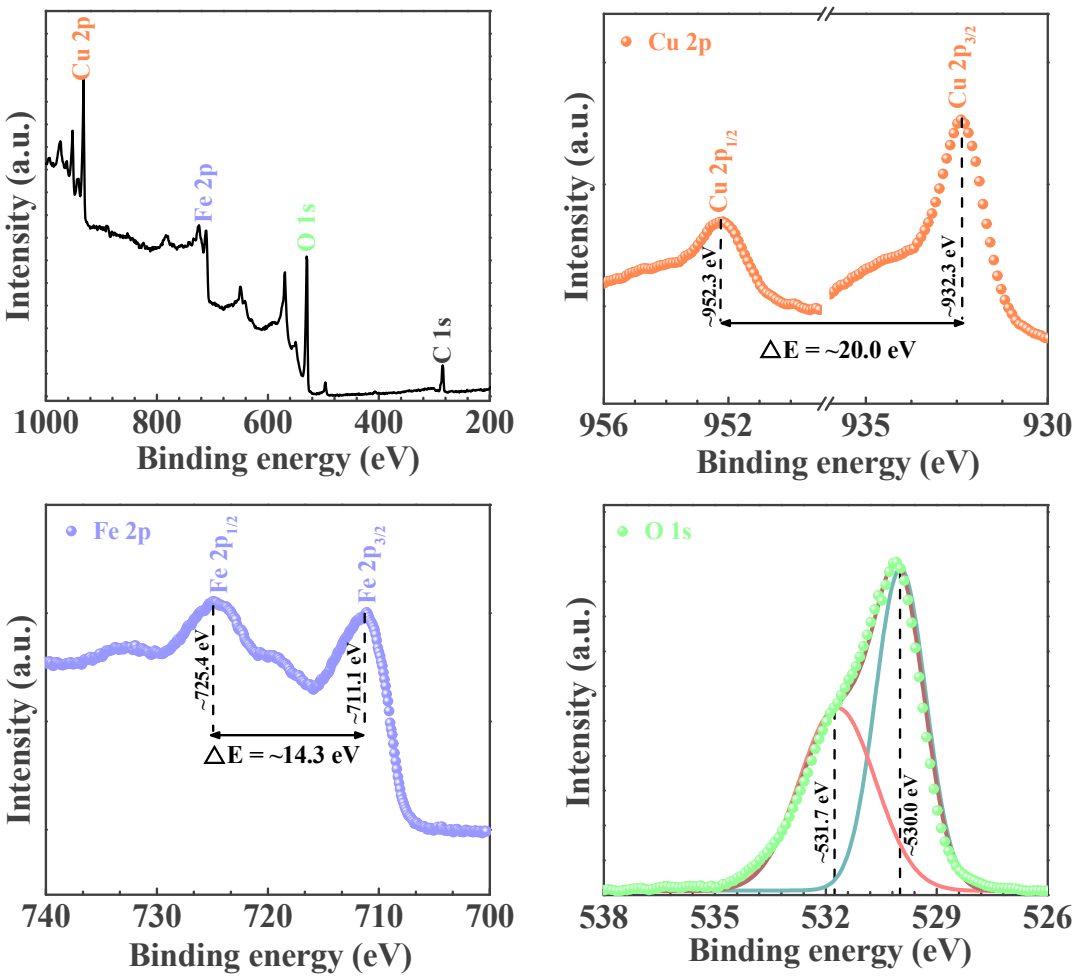

Fig. S2. XPS survey spectra and high resolution XPS spectra of Cu 2p, Fe 2p, and O 1s.

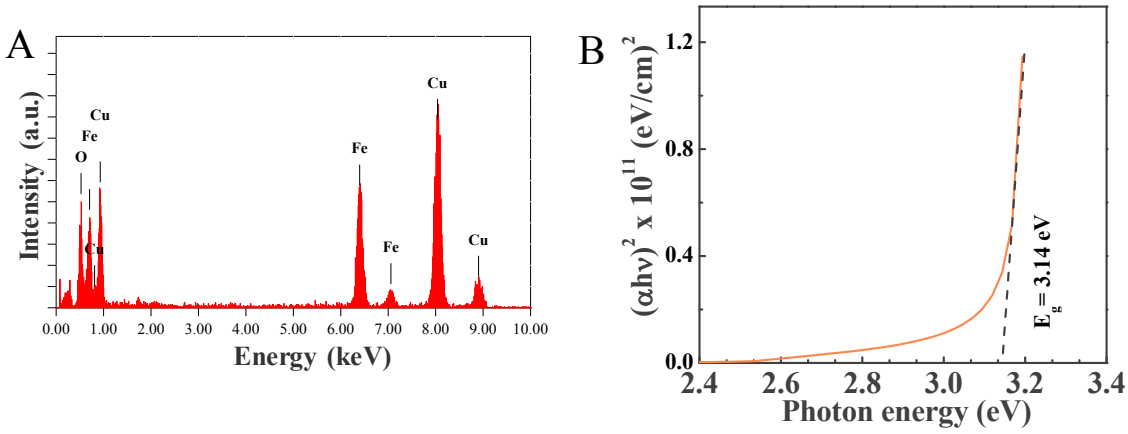

Fig. S3. (a) EDS spectrum of $CuFeO_2$ sample. (b) The extrapolated plot of $(\alpha h\nu)^2$ against hv obtained from the absorbance of $CuFeO_2$.

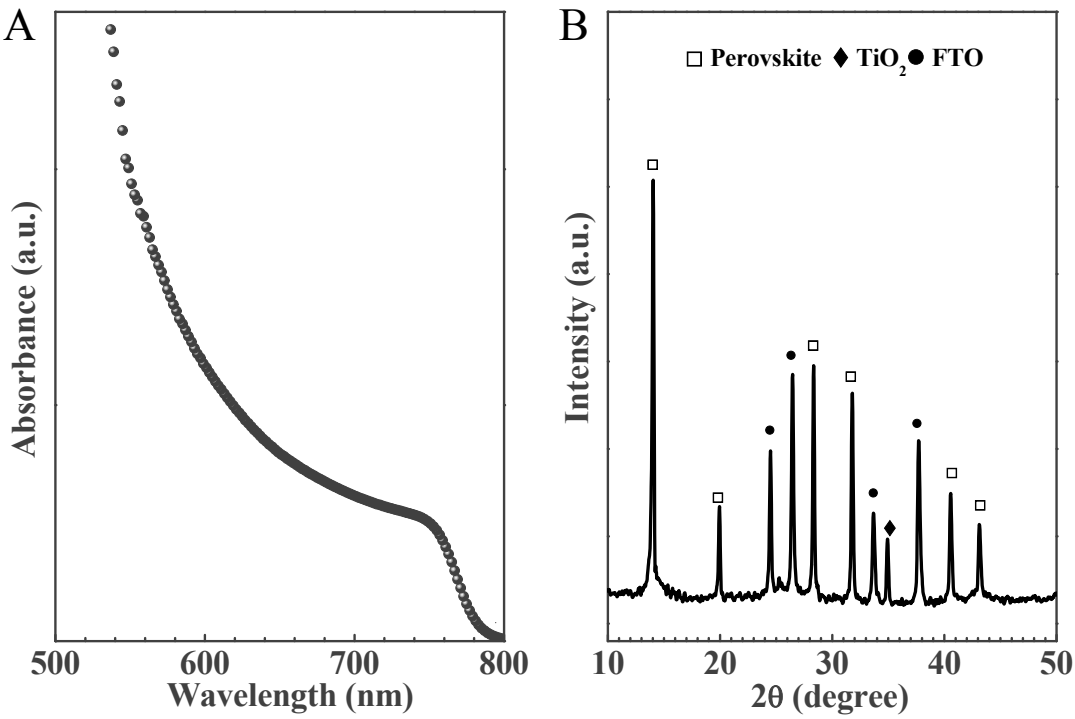

Fig. S4. (a) UV-vis absorption spectrum and (b) typical XRD pattern of perovskite film.

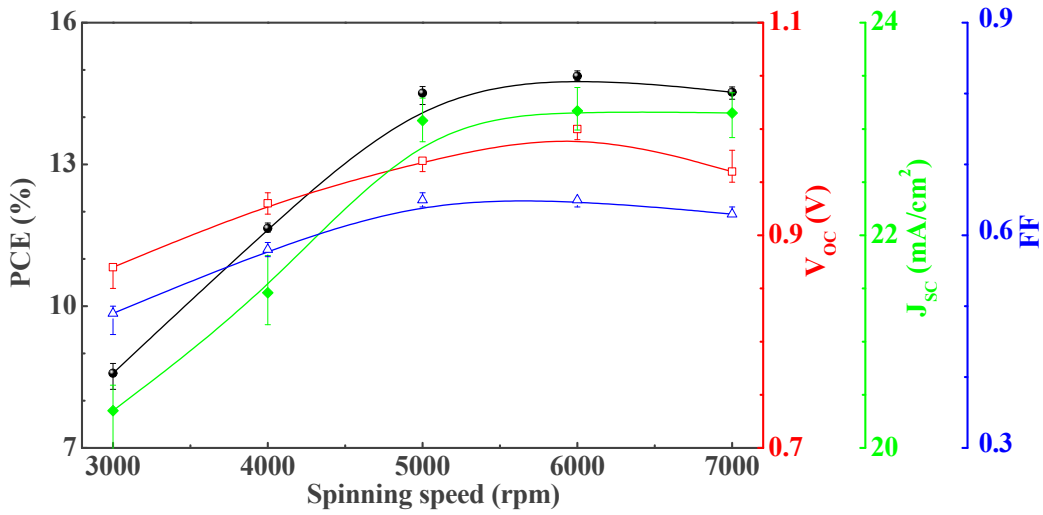

Fig. S5. *PCE* variations of PSCs as a function of spinning-speed during $CuFeO_2$ deposition.

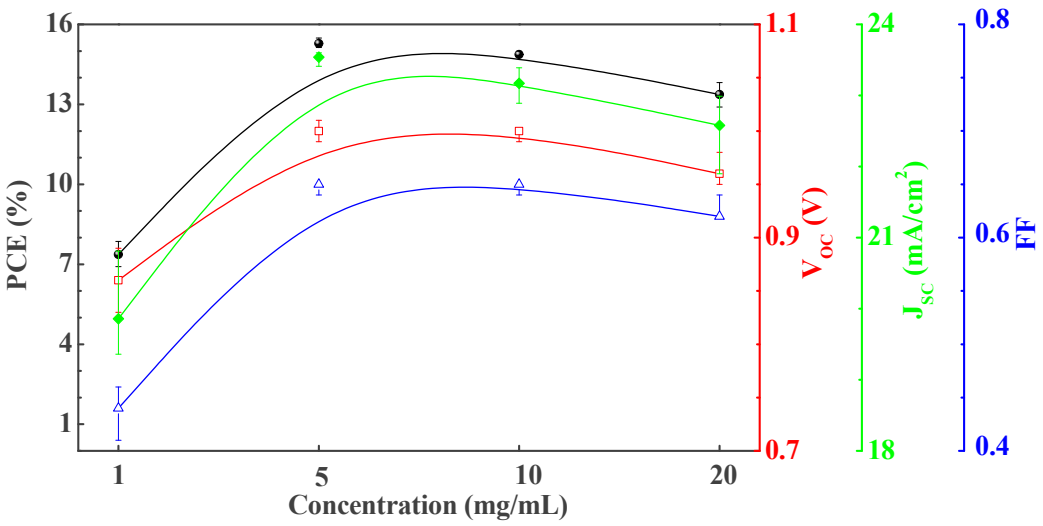

Fig. S6. *PCE* variations of PSCs as a function of $CuFeO_2$ concentration.

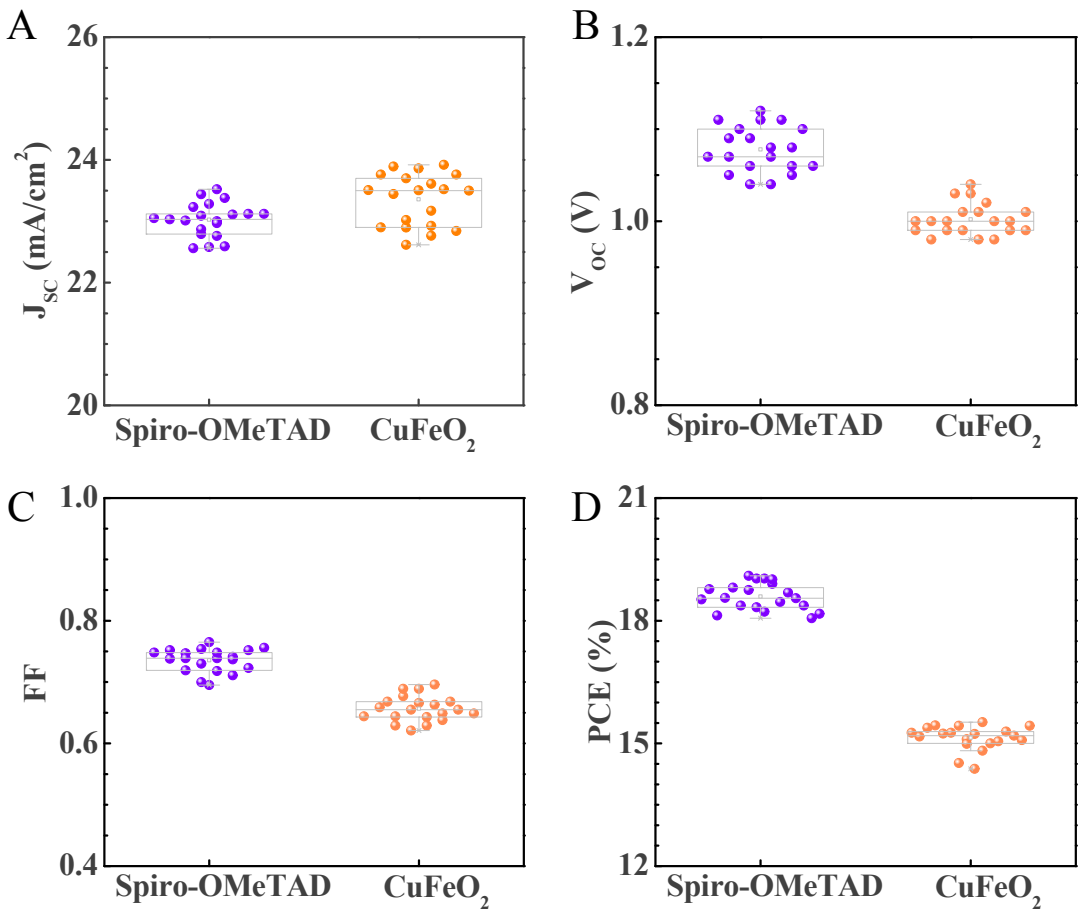

Fig. S7. PV metrics for devices employing spiro-OMeTAD (20 cells) and $CuFeO_2$ (20 cells) as HTMs: (a) J_{SC}, (b) V_{OC}, (c) *FF*, and (d) *PCE*.

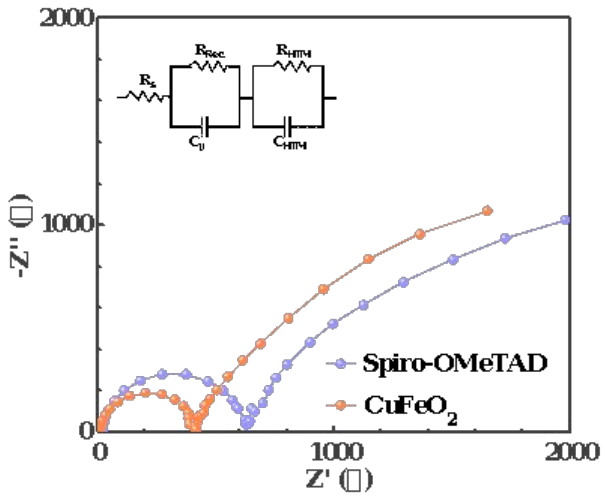

Fig. S8. EIS spectra (V_{app} = 0 mV) of the devices with spiro-OMeTAD and $CuFeO_2$ HTMs. The inset shows an equivalent circuit model employed for analysis.

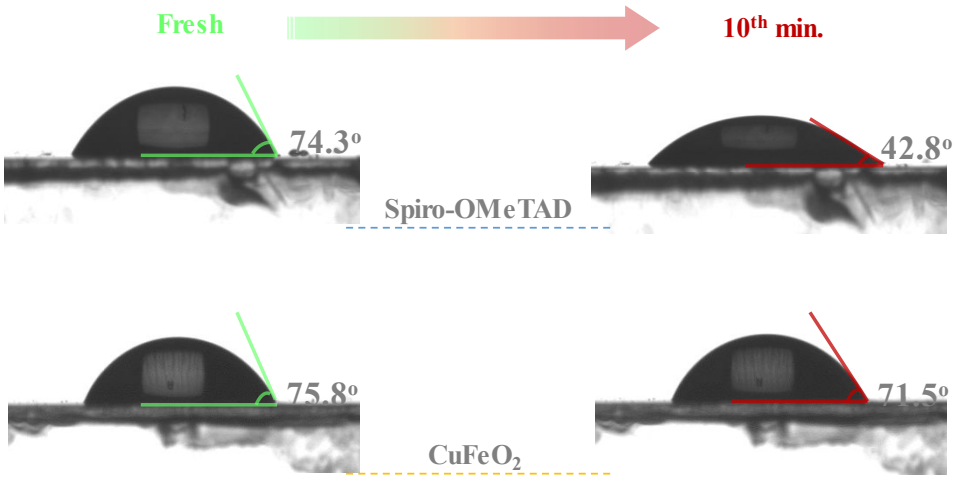

Fig. S9. Time dependent CAMs of spiro-OMeTAD and $CuFeO_2$ films on perovskite layer.